Importance of the structure of the RGD-containing loop in the disintegrins echistatin and eristostatin for recognition of αIIbβ3 and αvβ3 integrins

Mary Ann McLane[a,*], Senadhi Vijay-Kumar[b], Cezary Marcinkiewicz[a,c], Juan J. Calvete[d], Stefan Niewiarowski[a,c]

[a]*Sol Sherry Center for Thrombosis Research, Temple University School of Medicine, 3400 N. Broad Street, Philadelphia, PA 19140, USA*
[b]*Department of Biochemistry and Fels Research Institute, Temple University School of Medicine, Philadelphia, PA 19140 USA*
[c]*Department of Physiology, Temple University School of Medicine, Philadelphia, PA 19140, USA*
[d]*Tierarztlische Hochschule, Hannover-Kirchrode, Germany*

Received 3 June 1996

Abstract Echistatin and eristostatin are structurally homologous disintegrins which exhibit significant functional differences in interaction with various integrins. We hypothesized that this may reflect differences in the sequences of their RGD loops: ^{20}CKRARGDDMDDYC^{32} and ^{23}CRVARGDWNDDYC^{35}, respectively. Mapping of eristostatin peptides obtained by proteolytic digestion suggested that it has the same alignment of S–S bridges as echistatin. Synthetic echistatin D27W resembled eristostatin since it had increased platelet aggregation inhibitory activity, increased potency to block fibrinogen binding to αIIbβ3, and decreased potency to block vitronectin binding to αvβ3 as compared to wild-type echistatin. Since eristostatin and echistatin have a similar pattern of disulfide bridges, we constructed molecular models of eristostatin based on echistatin NMR coordinates. The RGD loops of eristostatin and echistatin D27W were wider than echistatin's due to the placement of tryptophan (rather than aspartic acid) immediately after the RGD sequence. We propose a hypothesis that the width and shape of the RGD loop are important ligand structural features that affect fitting of ligand to the binding pocket of αIIbβ3 and αvβ3.

Key words: RGD loop; Integrin αIIbβ3; Integrin αvβ3; Disintegrin; Disulfide bridge

1. Introduction

Since the early observations by Pierschbacher and Ruoslahti [1], it is well established that the arginine–glycine–aspartic acid (RGD) sequence plays a critical role for the recognition of a number of adhesive proteins by several integrins provided that this sequence occurs in an appropriate conformation. It is also established that the amino acid adjacent to the C-terminus of short RGD peptides alters its affinity to αIIbβ3 integrin, with tryptophan and phenylalanine increasing its affinity and hydrophilic amino acids decreasing its affinity [2].

Disintegrins are a family of naturally occurring proteins derived from viper venom which contain 49 to 84 amino acids including an RGD or KGD sequence and 8 to 14 cysteines linked by S–S bonds. Disintegrins bind with high affinity and inhibit the function of several integrins, including αIIbβ3, αvβ3 and α5β1. However, they show significant variation in their activity and selectivity [3]. NMR-derived structures for the disintegrins echistatin, kistrin and flavoridin reveal that they possess an RGD sequence at the apex of a mobile loop between two β strands of the protein, protruding 14–17Å from the protein core [4–6]. The RGD sequence is critical for the expression of biological activity of disintegrins since the substitution of Arg^{24} in echistatin [7] and Arg^{49} and Asp^{51} in kistrin [8] results in a considerable loss of disintegrin activity. The molecules also lose their function after reduction [9–11] and it appears that the pattern of intramolecular S–S bridges affects the activity of disintegrins [12]. Scarborough et al. [13] suggested that amino acids adjacent to the carboxy-terminal end of RGD determines selectivity of disintegrins. Disintegrins with RGDW and RGDNP sequences were quite selective in inhibiting native ligand binding to αIIbβ3 and αvβ3 integrin, respectively. More recently, Lu et al. [14] demonstrated that substitution of P42A and M46Q around the RGD domain of the neurotoxin dendroaspin alters its preferential anti-αIIbβ3 antagonism to that of the disintegrin elegantin, which appears to recognize a different ligand binding site in this receptor.

In our previous studies, we compared biological activities of two disintegrins, echistatin and eristostatin. These two disintegrins share 62% sequence identity and 69% sequence similarity, including eight cysteines [15] (Fig. 1). However, they show significant differences in their biological activities. Eristostatin is the most potent inhibitor of ADP-induced platelet aggregation among disintegrins, and it binds with the same high affinity to resting and activated platelets, whereas echistatin binding affinity to resting platelets is significantly lower than its binding affinity to ADP-activated platelets [15]. Echistatin inhibits more strongly the binding of vitronectin to immobilized αvβ3 than fibrinogen binding to immobilized αIIbβ3. Eristostatin is a more selective inhibitor of fibrinogen binding to αIIbβ3 than vitronectin binding to αvβ3 [16]. Echistatin reacts more extensively than eristostatin with HUVEC and with CHO cells transfected with αvβ3. Even if eristostatin binds to αvβ3 expressed on these cells, it does not interfere with their adhesion to vitronectin and fibronectin. In contrast, echistatin has a strong anti-adhesive property [17,18]. We hypothesized that the differences in biological activities of echistatin and eristostatin may reflect differences in the amino acid sequences of their RGD loops:

*Corresponding author. Fax: (1) (215) 707-4003

Abbreviations: RGD, arginine–glycine–aspartic acid; HUVEC, human umbilical vein endothelial cell; CHO, Chinese hamster ovary; NMR, nuclear magnetic resonance; PBST, phosphate buffered saline–Tween; RMS, root-mean-square

PII S0014-5793(96)00716-8

```
Eristostatin       QEEPCATGPCCRRCKFKRAGKVCRVARGDWNDDYCTGKSCDCPRNPWNG
Echistatin           ECESGPCCRNCKFLKEGTICKRARGDDMDDYCNGKTCDCPRNPHKGPAT
Echistatin D27W      ECESGPCCRNCKFLKEGTICKRARGDWMDDYCNGKTCDCPRNPHKGPAT
```

Fig. 1. Amino acid sequences of disintegrins with RGD loop in bold print. Amino acids are represented by single-letter code

^{20}CKRARGDDMDDYC^{32} and ^{23}CRVARGDWNDDYC^{35}, respectively. To confirm this hypothesis we first established that eristostatin has the same pattern of intramolecular S–S bridges as echistatin. We then compared the interaction of these two disintegrins and one echistatin analogue with purified receptors and developed molecular structures of these proteins.

2. Materials and methods

2.1. Materials

CHO cells transfected with αvβ3 were kindly provided by Drs. J. Loftus and M. Ginsberg, Scripps Research Institute, La Jolla, CA. Purified fibrinogen and polyclonal rabbit anti-fibrinogen (R97) were the gifts of Dr. Andrei Budzynski, Temple University, Philadelpha, PA. Anti-human vitronectin was from Gibco BRL. Alkaline phosphatase-conjugated secondary antibodies and purified human vitronectin were obtained from Sigma.

2.2. Preparation and characterization of disintegrins

Eristostatin and echistatin were purified into homogeneity from the crude venom of *Eristocophis macmahoni* and *Echis carinatus*, respectively, using two-step C-18 reversed-phase HPLC by the method of Williams et al. [19]. Synthetic echistatin$_{wt}$ and echistatin D27W were provided by Dr. Victor Garsky (Merck Sharp and Dohme Research Laboratories, West Point, PA). The amino acid sequences for these four proteins are shown in Fig. 1. The concentrations of eristostatin, echistatin and echistatin D27W that inhibited ADP-induced platelet aggregation (IC_{50}) determined as previously described [19] were 59±22 nM, 139±17 nM and 83±16 nM, respectively. Synthetic echistatin was identical in this functional assay to native echistatin.

2.3. Determination of disulfide arrangement in eristostatin

This was determined as previously described for echistatin [20]. Eristostatin (2 mg/ml in 100 mM NH_4HCO_3, pH 8.0) was digested with TPCK-trypsin at a protein/enzyme ratio of 100:1 (w/w) for 18 h at 37°C. Eristostatin (1 mg/ml in 250 mM oxalic acid) was also degraded in a degassed, sealed ampule for 5 h at 100°C [21]. The hydrolysates were lyophilized and the peptides were isolated by reversed-phase HPLC using a Lichrospher RP100C18 column (24×0.4 cm, 5 μm particle size) eluting at 1 ml/min with a mixture of 0.1% trifluoracetic acid in water (solution A) and acetonotrile (solution B) isocratically (100% A) for 5 min, followed by 0–30% B for 130 min, and 30–70% B for 40 min. Peptides were detected at 220 nm and collected manually. N-terminal sequence analyses were performed with an Applied Biosystems 470A sequencer following the manufacturer's instructions. Mass spectra were recorded with a mass spectrometer MAT 900 equipped with liquid secondary ion ionization system and a fast atom bombardment gun.

2.4. Preparation of isolated integrins (αIIbβ3 and αvβ3)

Platelet membrane αIIbβ3 complex was isolated from outdated platelets as described by Cook et al. [22]. αvβ3 was prepared from CHO cells transfected with human αvβ3 genes (VNRC3 cells), as described by Marcinkiewicz et al. [18].

2.5. Inhibitory activity of disintegrins in integrin ELISA

Purified integrins αIIbβ3 and αvβ3 (300 ng/well) were immobilized on 96-well microtiter plates overnight at 4°C in carbonate/bicarbonate buffer, pH 9.2. The plates were blocked with 5% (w/v) milk in PBST buffer. Varying concentrations of disintegrins (0–2000 pM) were mixed with ligand (fibrinogen or vitronectin, 1 μg) in buffer containing 20 mM Tris·HCl, pH 7.4, 150 mM NaCl, 1 mM $CaCl_2$, 1 mM $MgCl_2$, 1% (w/v) BSA, and incubated for 30 min at 37°C. After washing the wells with PBST, polyclonal anti-vitronectin or anti-fibrinogen was added. The amount of bound ligand was detected by the addition of goat anti-rabbit antibody conjugated to alkaline phosphatase, using nitrophenol phosphate as substrate. Testing of purified αIIbβ3 or αvβ3 binding to immobilized disintegrins was done as previously described [17].

2.6. Computer modeling of echistatin, eristostatin and echisD27W

The 3-dimensional structure of synthetic echistatin has been determined in aqueous solution by NMR [23]. A comparison of amino acid sequences between echistatin and eristostatin showed 62% identity and 69% sequence similarity (Fig. 1). All eight cysteine residues are completely conserved. In addition, we report here that the cysteine disulfide bridge pattern in eristostatin is identical to that in echistatin. The 3-dimensional NMR structure of echistatin reveals that the four disulfide bridges maintain its globular nature. Due to the high sequence identity, completely conserved cysteines and identical disulfide pattern, the overall folding of the polypeptide backbone of eristostatin would be very similar to that of echistatin. The 3-dimensional structure of eristostatin was built using the coordinates of an experimentally determined echistatin structure, using the computer program FRODO [24] on an ESV graphics system. The model was optimized for stereochemistry and then refined using the conjugate gradient energy minimization method of Powell [25]. The energy-minimized structure of eristostatin was further refined with a slow-cooling simulated annealing molecular dynamics procedure using X-PLOR [26]. Various molecular dynamics protocols used in developing the 3-dimensional structure of eristostatin, and in searching the conformational space for global minima, converged to the same 3-dimensional folding of the molecule. The orientation of residue side chain atoms was optimized using rotomer dictionary. In contrast to Pfaff et al. [27], who used such C_β atom distances to describe the RGD loop in a series of small

Table 1
Effect of variation in the disintegrin RGD loop on protein inhibitory activity with αIIbβ3 and αvβ3

Protein	IC_{50} (pM)		C_α distances (nm)	
	Fg/αIIbβ3	Vn/αvβ3	RGDX	XARGDX
Echistatin$_{wt}$	685±34	218±38	0.58	0.91
Eristostatin	115± 2	1671±46	0.82	0.70
Echistatin D27W	113± 5	616±29	0.85	0.88
Echistatin R22V/D27W	n.d.	n.d.	0.82	0.74

Proteins were tested for inhibitory activity with immobilized integrin in the presence of native ligand in an ELISA system. Distances between Cα positions of various residues of the RGD loop were obtained from computer modeling.

Eristostatin

```
1         10        20        30        40
.         .         .         .         .
QEEPCATGPCCRRCKFKRAGKVCRVARGDWNDDYCTGKSCDCPRNPWNG
```

TPCK-trypsin digest products:

1	QEEPCATGPCCR	12
14	CK	15
22	VCR	24
28	GDWNDDYCTGK	38
39	SCDCPR	44

Degradation products after incubation with 250 mM oxalic acid:

Fragment	$(M+H)^+$	Assignment	Cysteine pairing
E-19	794.4	^{4}PCATGP^{9} ^{14}CK^{15}	5-14
E-20	1192.3	^{22}VCRVAR^{27} ^{41}DCPR^{44}	
	1063.5	^{21}KVCRVAR^{27} ^{41}DC^{42} or ^{40}CD^{41}	23-(40/42)
E-22	1175.2	^{6}ATGPC^{10} or ^{5}CATGP^{9} ^{31}NDDYCT^{36}	(5/10)-35
E-23	934.2	^{21}KVCRV^{25} ^{41}DCP^{43}	
	835.3	^{21}KVCR^{24} ^{41}DCP^{43}	23-42
E-25	1104.4	^{19}AGKVCRV^{25} ^{42}CPR^{44}	23-42
E-29	1258.3	^{21}KVCRVA^{26} ^{42}CPRNP^{46}	
	1131.4	^{22}VCRVA^{26} ^{42}CPRNP^{46}	23-42

Fig. 2. Amino acid sequence of eristostatin and of peptides obtained by its digestion with TPCK-trypsin or degradation with 250 mM oxalic acid. The numbers of amino acid residues are marked on the top of eristostatin. The numbers at the left and right side of each peptide indicate its N- and C-terminal residues, respectively, and its localization within the eristostatin molecule. Peptides within brackets represent disulfide-binded polypeptides. $M+H^+$ indicates the molecular mass of the protonated molecular ion determined by mass spectrometry. In the right column, the cysteines contained in each substructure are indicated.

cyclic RGD peptides, we measured the distances between Cα atoms of selected residues in the RGD loop since they are part of the polypeptide backbone and are more descriptive of the position of the loop itself, rather than the more flexible side chains in the loop. In general, the methods employed here in developing the mutant models based on experimentally determined structures have shown a remarkable reproducibility with other proteins, such as HIV protease [28], and have been found to be consistent with X-ray crystallographic results.

3. Results and discussion

Fig. 2 summarizes the amino acid sequences of eristostatin

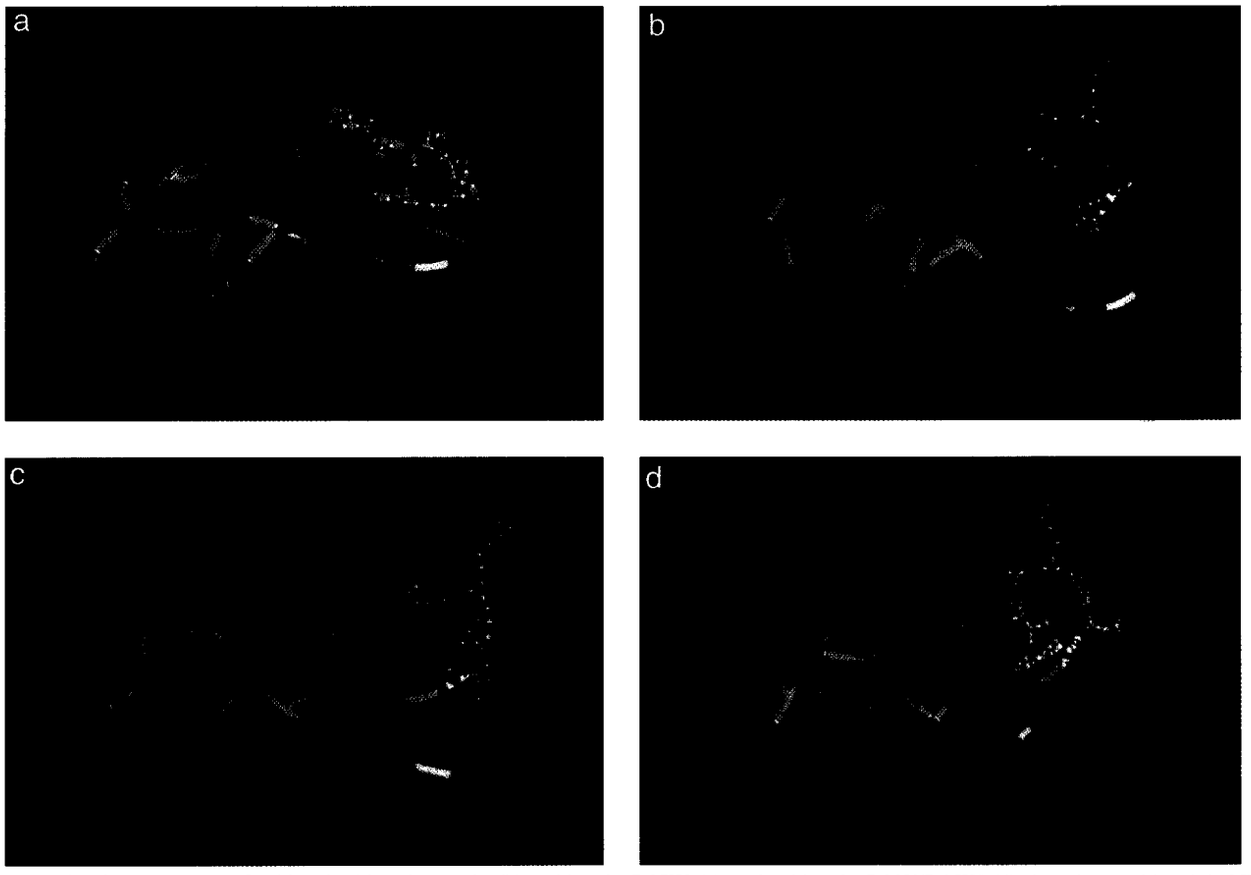

Fig. 3. Molecular structures of echistatin (a), eristostatin (b), echistatin D27W (c) and echistatin R22V/D27W (d), based on echistatin's NMR coordinates, built using the program FRODO, refined using conjugate gradient energy minimalization and simulated annealing molecular dynamics. Residue backbones are color-coded as follows: green, hydrophobic; blue, positively charged; red, negatively charged; yellow, containing sulfur; pink/pale blue, hydrophilic; white, tryptophan; magenta, asparagine/glutamine; cyan, glycine/proline. The side chains of the amino acids at the XARGDX loop are shown as ball-and-stick models.

and its peptides obtained by its digestion with TPCK-trypsin or degradation with oxalic acid, and subsequently analyzed by mass spectrometry. Although we cannot distinguish in fragment E-22 ($M+H^+ = 1175.2$) whether C35 is linked with C5 or C10, the bond C5–C35 can be ruled out because C5 forms a bridge with C14 in fragment E-19 ($M+H^+ = 794.4$). In addition, connection between C8–C37 should be deduced by exclusion. This structure is the same as for echistatin [20].

Table 1 shows that echistatin D27W had an inhibitory potency to block fibrinogen binding to immobilized αIIbβ3 that was higher than that of wild-type echistatin. On the other hand, this D27W substitution decreased the ability of echistatin to inhibit vitronectin binding to αvβ3, but to an intermediate level between wild-type echistatin and eristostatin. Similar results were obtained when we tested the binding of αIIbβ3 and αvβ3 to immobilized eristostatin, echistatin and echistatin D27W (data not shown).

To explain the differences in biological activities among both disintegrins and echistatin D27W, we developed molecular structures for each protein (Fig. 3), based on echistatin NMR coordinates. Echistatin is predominantly a loop structure with four nonstandard turns and has no secondary structural elements. The folding force is largely due to the four disulfide bridges between eight cysteine residues. The structure does not have a hydrophobic core. The three loops and the N-terminal part of the molecule are held together through four cystine bridges (Fig. 3a). The model for eristostatin (Fig. 3b) developed through homology modeling, refined by energy minimization and molecular dynamics, compares well with the echistatin structure. The rms deviations in Cα coordinates between the two proteins is 3.3 Å. Although the overall folding in these two molecules is very similar, the large rms deviations in Cα coordinates is due to the difference in the width of the RGD loop and the C-terminus of the protein. The total energy calculated by considering various interactions (electrostatic, van der Waal's, etc.) for echistatin is −1112 kcal, and for eristostatin is −1092 kcal. In the development of this eristostatin structure from the experimentally determined structure of echistatin, various protocols of molecular dynamics simulation were used, all resulting in the same global fold. The presence of tryptophan (W30), which is a large hydrophobic residue, following the RGD sequence in eristostatin makes the RGD loop significantly wider than the RGD loop in echistatin, which has aspartic acid (D27) following the RGD sequence. The rms deviations between the Cα positions of the sequence XARGDX in eristostatin and echistatin is 2.1 Å.

The model developed for the echistatin analog D27W shows a similar increase in the width of the RGD loop, shown in Fig. 3c. In addition, the two residues Val and Trp

(*V*ARGD*W*) in eristostatin's RGD loop clearly show hydrophobic interactions between them, which are important for the additional stability of the RGD loop. The structure of the double mutant of echistatin (R22V/D27W), developed using the same molecular dynamics methods, demonstrated a shape and size of the RGD loop which is very similar to that of eristostatin. The rms deviations in Cα coordinates of the sequence VARGDW in eristostatin and echistatin R22V/D27W is 0.9 Å.

Table 1 shows that eristostatin and echistatin D27W have the same width of the RGD loop (measured as the distance between Cα of RGDX) which is greater than the width of the echistatin loop. This width of the loop seems to correlate with the binding affinity to αIIbβ3 since both eristostatin and echistatin D27W have similar inhibitory effect on the binding of αIIbβ3 to fibrinogen and similar platelet aggregation inhibitory activity. The width of eristostatin's RGD loop compared with that of echistatin depends on the placement of tryptophan (rather than aspartic acid) immediately after the RGD sequence. However, the ability of echistatin D27W to inhibit binding of vitronectin to αvβ3 was intermediate between that of echistatin or eristostatin. Interestingly, the shape of the RGD loop (measured as the distance between Cα of XARGDX) is very similar in echistatin and echistatin D27W. The shape of the loop was ultimately determined by the two amino acid residues N-terminal to the RGD sequence: valine in eristostatin and arginine in both echistatin$_{wt}$ and echistatin D27W. This was also confirmed by creating a computer model of a second echistatin variant. Replacing R22 in echistatin with valine and D27 with tryptophan gave an echistatin molecule which could be superimposed on eristostatin (Fig. 3d and Table 1). Since echistatin D27W is less selective to αvβ3 than wild-type echistatin, but is still much more selective than eristostatin (Table 1), it is possible that the second substitution (R22V) in echistatin will bestow comparable selectivity as eristostatin. On the basis of our studies, we propose a hypothesis that while the width of the RGD loop is an important ligand structural feature creating an optimal fit to the binding pocket of αIIbβ3, the shape of the loop, influenced by the amino acids nearer the disulfide bridge itself, is a major determinant in whether an RGD-containing ligand will bind to the vitronectin receptor. This hypothesis has to be confirmed experimentally by creating an echistatin double mutant, R22V/D27W, and assessing its affinity to αvβ3 in comparison to both wild-type echistatin and eristostatin. Our data confirm and extend the observations of Pfaff et al. [27], who have shown that larger distances between Cβ atoms of arginine and aspartic acid in cyclic RGD peptides imparts a selectivity for αIIbβ3 versus either αvβ3 or α5β1 binding.

Acknowledgements: We are grateful to Dr. Mark Ginsberg for the transfected cells, Dr. Victor Garsky for the synthetic echistatin proteins and Dr. Andrei Budzynski for the fibrinogen and anti-fibrinogen antibody. We are also indebted to Dr. Yuqin Wang for preparation of natural echistatin and eristostatin, and Mariola Marcinkiewicz for the solid-phase assays and the preparation of purified receptor. This investigation was supported by NIH Grants HL45486 (S.N.), an NIH postdoctoral traineeship 1T32HL0777701 (M.A.M.) and a postdoctoral fellowship from the American Heart Association, Southeastern Pennsylvania Affiliate (M.A.M.).

References

[1] Pierschbacher, M.D. and Ruoslahti, E. (1984) Nature 309, 30–33.
[2] Tranqui, L., Andrieux, A., Hudry-Clergeon, G., Ryckeweart, J.-J., Soyez, S., Chapel, A., Ginsberg, M.H., Plow, E.F. and Marguerie, G. (1989) J. Cell Biol. 108, 2519–2527.
[3] Niewiarowski, S., McLane, M.A., Kloczewiak, M. and Stewart, G.J. (1994) Sem. Hematol. 31, 289–300.
[4] Saudek, V., Atkinson, R.A. and Pelton, J.T. (1991) Biochem. 30, 7369–7372.
[5] Adler, M., Lazarus, R.A., Dennis, M.S. and Wagner, G. (1991) Science 253, 445–448.
[6] Senn, H. and Klaus, W. (1993) J. Mol. Biol. 232, 907–925.
[7] Garsky, V.M., Lumma, P.K., Freidinger, R.M., Pitzenberger, S.M., Randall, W.C., Veber, D.F., Gould, R.J. and Friendman, P.A. (1989) Proc. Natl. Acad. Sci. 86, 4022–4026.
[8] Dennis, M.S., Carter, P. and Lazarus, R.A. (1993) Proteins 15, 312–321.
[9] Huang, T.-F., Holt, J.C., Lukasiewicz, H. and Niewiarowski, S. (1987) J. Biol. Chem. 262, 16157–16163.
[10] Gan, Z.R., Gould, R.J., Jacobs, J.W., Friedman, P.A. and Polokoff, M.A. (1988) J. Biol. Chem. 263, 19827–19832.
[11] Scarborough, R.M., Rose, J.W., Hsu, M.A., Phillips, D.R., Fried, V.A., Campbell, A.M., Nannizzi, L. and Charo, I.F. (1991) J. Biol. Chem. 266, 9359–9362.
[12] Calvete, J.J., Schäfer, W., Soszka, T., Lu, W., Cook, J.J., Jameson, B.A. and Niewiarowski, S. (1991) Biochemistry 30, 225–5229.
[13] Scarborough, R.M., Rose, J.W., Naughton, M.A., Phillips, D.R., Nannizzi, L., Arfsten, A., Campbell, A.M. and Charo, I.F. (1993) J. Biol. Chem. 268, 1958–1065.
[14] Lu, X., Rahman, S., Kakkar, V.V. and Authi, K.S. (1996) J. Biol. Chem. 271, 1–6.
[15] McLane, M.A., Kowalska, M.A., Silver, L., Shattil, S.J. and Niewiarowski, S. (1994) Biochem. J. 301, 429–436.
[16] Pfaff, M., McLane, M.A., Beviglia, L., Niewiarowski, S. and Timpl, R. (1994b) Cell Adhes. Comm. 2, 491–501.
[17] Juliano, D., Wang, Y., Marcinkiewicz, C., Rosenthal, L.A., Stewart, G.J. and Niewiarowski, S. (1996) Exp. Cell Res. 225, in press.
[18] Marcinkiewicz, C., Rosenthal, L.A., Mosser, D.M., Kunicki, T.J. and Niewiarowski, S. (1996) Biochem. J. 317, in press.
[19] Williams, J., Rucinski, B., Holt, J. and Niewiarowski, S. (1990) Biochem. Biophys. Acta 1039, 81–89.
[20] Calvete, J.J., Wang, Y., Mann, K., Schäfer, W., Niewiarowski, S. and Stewart, G. (1992) FEBS Lett. 309, 316–320.
[21] Bauer, M., Sun, Y., Degenhardt, C. and Kozikowski, B. (1993) J. Prot. Chem. 12, 759–764.
[22] Cook, J.J., Trybulec, M., Lasz, E.C., Khan, S. and Niewiarowski, S. (1992) Biochim. Biophys. Acta 1119, 312–321.
[23] Dalvit, C., Widmer, H., Bovermann, G., Breckenridge, R. and Metternich, R. (1991) Eur. J. Biochem. 202, 315–321.
[24] Jones, T.A. (1978) J. Appl. Crystallogr. 11, 268–272.
[25] Powell, M.J.D. (1977) Math. Progr. 12, 241–254.
[26] Brünger, A.T., Krukowski, A. and Erickson, J.W. (1990) Acta Cryst. A46, 585–593.
[27] Pfaff, M., Tangemann, K., Müller, B., Gurrath, M., Müller, G., Kessler, H., Timpl, R. and Engel, J. (1994a) J. Biol. Chem. 269, 20233–20238.
[28] Weber, I.T. (1990) Prot: Struct. Funct. Genet. 7, 172–184.